WATER RESOURCES RESEARCH, VOL. 28, NO. 12, PAGES 3129–3134, DECEMBER 1992

The Unstable Surface Layer Above Forest: Regional Evaporation and Heat Flux

WILFRIED BRUTSAERT

School of Civil and Environmental Engineering, Cornell University, Ithaca, New York

MARC B. PARLANGE

Hydrologic Science, Department of Land, Air, and Water Resources and Department of Agricultural Engineering, University of California, Davis

Radiosonde measurements above the heterogeneous forest of the Landes region in southwestern France provided vertical profiles of potential temperature and specific humidity in the atmospheric boundary layer. For all of the 62 profiles analyzed under unstable atmospheric conditions a surface sublayer could be identified within which the Monin-Obukhov similarity was consistent with the regional surface fluxes of sensible heat and latent heat (evaporation). For the potential temperature the vertical extent of this sublayer was found to be 41 (± 30) ≤ $(z - d_0)/z_0$ ≤ 130 (± 49), where z_0 = 1.2 m is the roughness height and d_0 = 6.0 m is the displacement height; for the specific humidity it was 48 (± 36) ≤ $(z - d_0)/z_0$ ≤ 153 (± 63). These results show that irregular forest surfaces are not anomalous, as regards the lower limit of the surface layer in comparison with surfaces with smaller roughness. The surface fluxes derived from the profile measurements were compared with flux measurements obtained by means of an eddy correlation system atop a 29 m mast, some 9 m above a mature section of forest some 4.5 km away from the launching site of the radiosondes; these independent measurements were made by a team from the Institute of Hydrology (Wallingford, England). On average, these two types of estimates were in good agreement. For the sensible heat flux the correlation coefficient was r = 0.75. For the evaporation rate it was r = 0.66. For the evaporation obtained by means of the energy budget from the sensible heat flux it improved to r = 0.82. The profile-derived fluxes did not compare as favorably with corresponding flux values measured above agricultural crops in clearings. This confirms that the forest was the dominant surface at the regional scale.

1. INTRODUCTION

The atmospheric boundary layer (ABL) is one of the key elements in the description and analysis of hydrologic phenomena at scales appropriate for watersheds and river basins. Turbulent boundary layers under neutral and unstable conditions typically have vertical to horizontal turbulence scale ratios of around 1/10 to 1/100. Thus with a characteristic thickness of the order of 10^2–10^3 m, through the integrating power of the turbulence, the structure of a well-developed ABL is the result of boundary conditions and surface exchange processes over upwind distances, or fetches, of the order of some 10 km or more. Such horizontal distances are similar to those characterizing the sizes of upland source areas in catchment hydrology.

Most research on the ABL in the past has dealt with the inner region or surface sublayer. This sublayer is considered to be far enough from the surface that the detailed structure of the surface cannot be detected in the turbulence but yet close enough that such factors as the rotation of the earth, large-scale pressure gradients, boundary layer entrainment, unsteadiness, the weather, etc. have no direct effect on the flow. It is now generally accepted that over uniform surfaces the similarity scheme of *Monin and Obukhov* [1954] provides a good description of the mean (in the turbulence sense) concentration of any admixture of the flow. In the case of momentum, sensible heat, and water vapor one can write

$$V = \frac{u_*}{k}\left[\ln\left(\frac{z - d_0}{z_0}\right) - \psi_m\left(\frac{z - d_0}{L}\right)\right] \tag{1}$$

$$\theta_r - \theta = \frac{H}{k u_* \rho c_p}\left[\ln\left(\frac{z - d_0}{z_r - d_0}\right) - \psi_h\left(\frac{z - d_0}{L}\right) + \psi_h\left(\frac{z_r - d_0}{L}\right)\right] \tag{2}$$

$$q_r - q = \frac{E}{k u_* \rho}\left[\ln\left(\frac{z - d_0}{z_r - d_0}\right) - \psi_v\left(\frac{z - d_0}{L}\right) + \psi_v\left(\frac{z_r - d_0}{L}\right)\right] \tag{3}$$

where V is the mean wind speed, $u_* = (\tau_0/\rho)^{1/2}$ is the friction velocity, τ_0 is the surface shear stress, ρ is the density of the air, k = 0.4 is von Karman's constant, z is the height above the ground or the base level of the roughness elements, z_0 is the roughness height, d_0 is the displacement height, θ is the potential temperature, c_p is the specific heat at constant pressure, and q is the specific humidity; the subscript r denotes a reference level within the surface sublayer, and H and E are the specific surface fluxes of sensible heat and water vapor, respectively.

The ψ symbols denote the integral Monin-Obukhov stability correction functions which depend on $\nu = (z - d_0)/L$; L is the Obukhov length, defined by

Paper number 92WR01860
0043-1397/92/92WR-01860$05.00

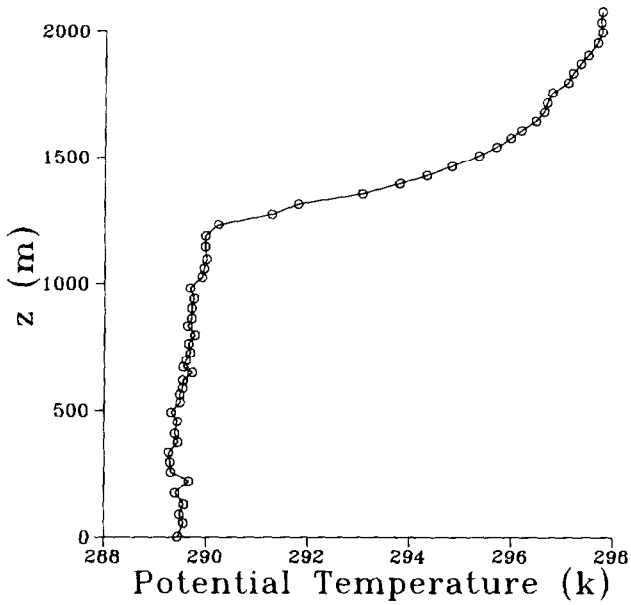

Fig. 1. Example of potential temperature profile for flight 201 (1120 UT; June 11, 1986).

$$L = -\frac{u_*^3}{kg[H_v/(\rho c_p T_a)]} \tag{4}$$

where $H_v = H + 0.61 T_a c_p E$ is the specific flux of virtual sensible heat at the surface and T_a is the air temperature near the ground. These similarity functions, which are usually presented in differential form, that is, for the vertical concentration gradients, have been the subject of numerous experimental studies. The Businger-Dyer formulation for sensible heat and water vapor [e.g., *Businger*, 1988; *Högström*, 1988; *Dyer*, 1974] is widely accepted on the basis of field scale studies. With $k = 0.4$ the integral form of the formulation for unstable conditions can be written as

$$\psi_c = 2 \ln [(1 + u^2)/2] \tag{5}$$

where the subscript c can represent h and v for heat and water vapor, respectively, and

$$u = (1 - 16y)^{1/4} \tag{6}$$

Equation (6) is also close to the formulation obtainable from the proposal by *Kader and Yaglom* [1990] [see *Brutsaert*, 1992].

Over the past half century much research has been devoted to ABL surface layer similarity; but its applicability in hydrology in relation to evaporation is still not well understood, and a number of uncertainties remain. In particular, this is the case for surfaces which are not quite homogeneous and uniform, as well as for surfaces with tall vegetation and forest. The first of these two outstanding issues is encountered in almost all applications of surface layer similarity to the natural environment. Uniform surfaces are the exception, and little is known about the robustness of (1)–(6) for surfaces whose uniformity is less than perfect. The second issue, that of the possible failure or, at least, inadequacy of standard surface layer similarity above forest, was raised by *Thom et al.* [1975]; their experimental findings are now sometimes referred to as the "Thetford anomaly" [e.g., *Raupach*, 1979; *Shuttleworth*, 1989]. The proper interpretation of this and other [e.g., *Garratt*, 1978] evidence has been the subject of some discussion [e.g., *Hicks et al.*, 1979; *Raupach et al.*, 1979; *Garratt*, 1979]. Still, the present consensus appears to be that within a transition layer immediately above the forest canopy, standard surface layer similarity as given by (1)–(6) is not valid and that it is valid only higher up. *Garratt* [1980] has proposed an empirical modification for the flux profile functions in this transition layer. However, there is apparently still no agreement on the thickness of the transition layer, that is, on the lower height limit of the surface sublayer. Nor is it clear whether surfaces covered with tall vegetation and forest are anomalous in this regard, as compared to surfaces with smaller roughness. This paper aims to shed some light on these two issues. The main objective here is to assess the relevance of surface layer similarity to regional evaporation and related processes. This is done by testing (2)–(6) with profile data and surface fluxes measured during HAPEX-MOBILHY over heterogeneous, nonuniform forest in southwestern France. The analysis focuses on unstable conditions because the surface fluxes tend to be the largest when there is surface heating.

2. Field Measurements

The measurements were recorded in the forested region of the Landes, as part of HAPEX-MOBILHY (Hydrologic-Atmospheric Pilot Experiment—Modélisation du Bilan Hydrique), which had its main observing period from May 6 to July 14, 1986. General descriptions of the larger experiment have been presented by *André et al.* [1986, 1988]. The atmospheric profiles of V, θ, and q were obtained with radiosondes, which were released from a site at approximately 00°03'W, 44°08'N near Lubbon. The Landes Forest has a nearly flat topography; roughly 65% of the general experimental area is occupied by pine forest stands, in different stages of growth, and the remaining 35% by clearings. The linear dimensions of these clearings and of the different stands of uniform trees are typically of the order of 10^2 to 10^3 m. The surface roughness and the displacement height of the general experimental area were determined in earlier studies [*Parlange and Brutsaert*, 1989, 1990] to be $z_0 = 1.2$ m and $d_0 = 6.0$ m. Further details on the experimental area and the radiosonde system were presented by *Brutsaert et al.* [1989] and *Parlange and Brutsaert* [1989].

From 405 available radiosonde flights, 62 unstable ones were considered suitable for the analysis in the present investigation on the basis of the following criteria: eddy correlation flux measurements (see below) were available, and all three components of the radiosounding (wind speed, temperature, and humidity) were measured. In order to capture possible effects of the diurnal evolution of the ABL in the analysis, the 62 profiles were subdivided into three classes, namely, (1) morning profiles with the height of the bottom of the inversion h_i below 500 m, (2) those with $h_i >$ 500 m but prior to 1530 solar time, and (3) those later in the afternoon after 1530. The heights of the mixed layer h_i were determined from the temperature profiles with the criterion $dT/dp \leq 4c/100$ hPa. Examples of the potential temperature and specific humidity are shown for flight 201 in Figures 1 and 2, respectively.

The surface flux data H and LE ($= L_v E$, in which L_v is the latent heat of evaporation) used in the present investiga-

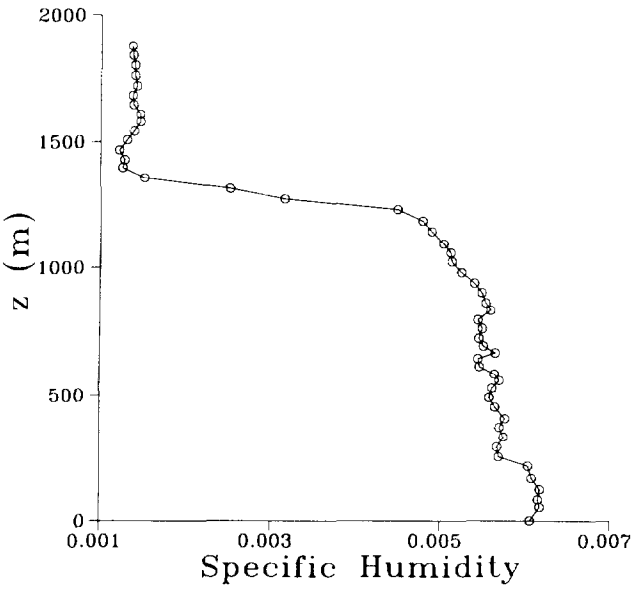

Fig. 2. Example of specific humidity profile for flight 201 (1120 UT; June 11, 1986).

tion to test (2)–(6) were obtained from hourly values measured by means of eddy correlation methods on a mast at about 9 m above the surrounding forest canopy. This site was located some 4.5 km to the southwest of the radiosonde release point. Details of this flux measuring system have been presented by *Gash et al.* [1989]. The values of the sensible and latent heat fluxes H_s and LE_s ($\equiv L_e E_s$) measured by this system were interpolated to the release times of the sondes. As described elsewhere [*Brutsaert et al.*, 1989], in addition to this flux station operated on the mast in the forest, two flux stations were operated in the oat and Indian corn (maize) fields in the large clearing at the radiosonde launching point. These flux data will also be compared below with those obtained by the Monin-Obukhov analysis.

3. Calculation of Regional Surface Fluxes

3.1. *Linear Regression With Profile Equations*

Equations (2) and (3) can be conveniently recast as follows to calculate the surface fluxes H and E by least squares linear regression:

$$\theta = a\left[\ln (z - d_0) - \psi_c\left(\frac{z - d_0}{L}\right)\right] + b \qquad (7)$$

$$q = c\left[\ln (z - d_0) - \psi_c\left(\frac{z - d_0}{L}\right)\right] + d \qquad (8)$$

where the slopes are $a = -H/(ku_*\rho c_p)$ and $c = -E/(ku_*\rho)$ and the intercepts are $b = \theta_r - a\,[\ln (z_r - d_0) - \psi_c((z - d_0)/L)]$ and $d = q_r - c\,[\ln (z_r - d_0) - \psi_c((z_r - d_0)/L)]$. For any selected set of adjacent points in the surface sublayer of a given profile, namely, $\theta = \theta(z)$ and $q = q(z)$, the values of H and E can be obtained from the slopes a and c, respectively, provided u_* and L are known. The values of u_* used for this purpose were derived from the corresponding wind profiles by *Parlange and Brutsaert* [1992]. The values of L used in (7) and (8) were calculated by means of (4) with these u_* values and with H_c and E_c obtained from the eddy correlation measurements. Of course, it is also possible to calculate L through an iteration process of (4), (7), and (8) with successive approximations of H and E; this alternative was also carried out in this study, but the results are practically the same and are therefore not considered further.

3.2. *Identification of Surface Sublayer*

Visual inspection of the radiosonde profiles can give a general idea of the extent of the surface sublayer or the inner region. In the case of the potential temperature profile the positive sensible heat flux at the land surface and the negative sensible heat flux at the inversion result in a superadiabatic to adiabatic lapse rate for the inner region and in an adiabatic to subadiabatic lapse rate for the outer region (e.g., Figure 1). This difference between the inner and outer regions is not as clear for the humidity profile (e.g., Figure 2); the water vapor flux at the inversion tends to be positive, so that the q gradient is usually negative throughout the ABL.

In practice, however, it is not easy to know a priori exactly where the Monin-Obukhov analysis should be applied. Radiosoundings often yield noisy profiles, so that regression analysis by means of (7) and (8) is very sensitive to the data point selection. Inclusion or omission of a data point can result in vastly different surface fluxes. The sampling times of the radiosonde sensors (a few seconds) and the passage times of the sondes through the ABL (a few minutes) are short compared to the integral time scales of the turbulence (15 to 30 min). Thus the sonde measurements reflect not only mean structure but also small-scale turbulence. As a result, the optimal performance of (7) and (8) does not occur over the same height range for each individual profile. After several trials it was possible to establish simple rules for selection of the optimal point range.

In the case of potential temperature the maximal range was chosen such that the H value calculated by means of (7) would have a reasonable magnitude; "reasonable" means that it is smaller than the net radiation and larger than a lower limit, which was taken as 40 W/m^2 for the morning flights, 100 W/m^2 for the midday flights, and 70 W/m^2 for the late afternoon. In Figure 3 the selected range is indicated by the solid points. This example illustrates that typically there is a fairly clear break between the inner and the outer region, so that point selection generally was straightforward.

The mean height ranges (and standard deviations) are, for θ,

Ten morning flights

$$59(\pm 38) \le z \le 130(\pm 47)\ \text{m};\ (\le 0.35(\pm 0.16)h_i)$$

Thirty-six midday flights

$$58(\pm 31) \le z \le 186(\pm 48)\ \text{m};\ (\le 0.18(\pm 0.07)h_i) \qquad (9)$$

Sixteen afternoon flights

$$69(\pm 36) \le z \le 154(\pm 56)\ \text{m};\ (\le 0.11(\pm 0.04)h_i)$$

All 62 flights

$$61(\pm 33) \le z \le 169(\pm 54)\ \text{m};\ (\le 0.19(\pm 0.11)h_i)$$

The upper limits are also given as fractions of the mixed layer height. The extent of the inner region above the Landes region is apparently not dependent on the time of day, and the height of the mixed layer h_i is probably not a good scale.

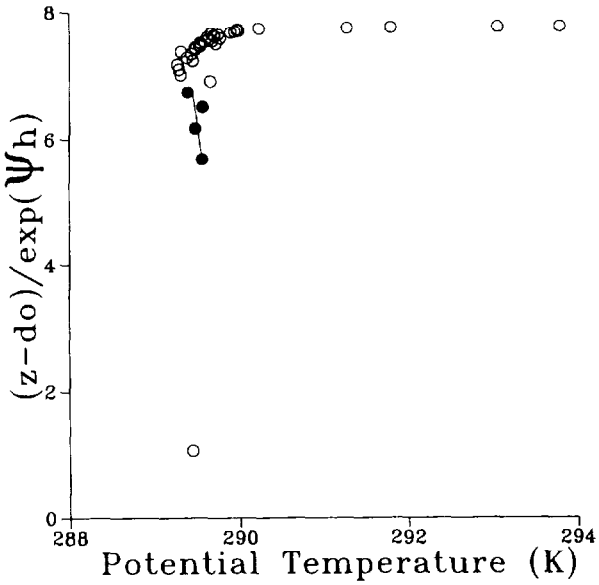

Fig. 3. Same as Figure 1 but ordinate is scaled with independent variable of linear regression with (7) (solid points indicate surface sublayer).

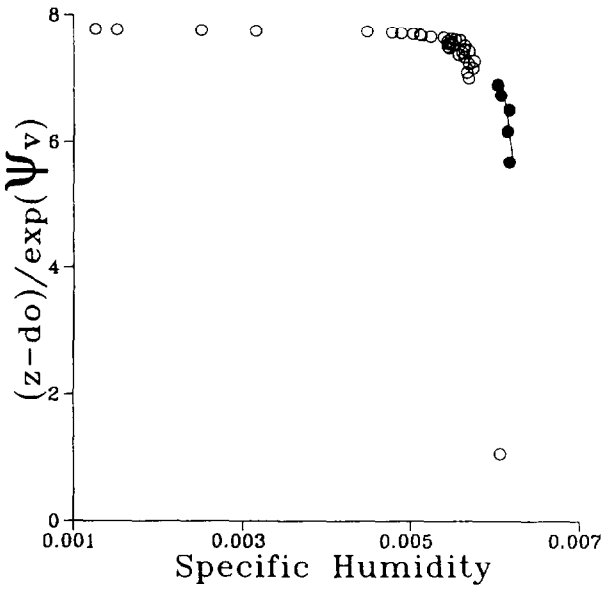

Fig. 4. Same as Figure 2 but ordinate is scaled with independent variable of linear regression with (8) (solid points indicate surface sublayer).

As suggested by (1), (2), and (3), the roughness length z_0 may be more appropriate; scaled this way the dimensionless height range for all flights is

$$46(\pm 28) \leq (z - d_0)/z_0 \leq 136(\pm 45) \qquad (10)$$

For the specific humidity the inner region may appear to be more difficult to identify than the θ range since, as illustrated in Figure 2, the q profile usually decreases throughout the ABL. Nevertheless, in the case of specific humidity the height range could generally be selected by using the same rule as for θ, namely, the maximal number of contiguous points such that LE calculated by means of (8) did not fall outside the same bounds imposed on H. For a large number of q profiles the identification of the range was relatively straightforward; these were profiles which displayed clear breaks, that is, sudden increases or decreases in q in an otherwise smoothly decreasing profile, so that inclusion of additional points above or below the chosen range resulted in unrealistic LE values. Figure 4 illustrates the selected range for flight 201 as the solid points.

For the q profiles the selected ranges had the following mean values (and standard deviations):

Ten morning flights

$$53(\pm 30) \leq z \leq 146(\pm 67) \text{ m}; \ (\leq 0.50(\pm 0.32)h_i)$$

Thirty-six midday flights

$$58(\pm 25) \leq z \leq 183(\pm 67) \text{ m}; \ (\leq 0.21(\pm 0.10)h_i)$$

Sixteen late flights (11)

$$66(\pm 47) \leq z \leq 198(\pm 76) \text{ m}; \ (\leq 0.14(\pm 0.06)h_i)$$

All 62 flights

$$59(\pm 32) \leq z \leq 181(\pm 70) \text{ m}; \ (\leq 0.24(\pm 0.19)h_i)$$

In dimensionless form the range for all flights is

$$44(\pm 27) \leq (z - d_0)/z_0 \leq 146(\pm 58) \qquad (12)$$

These mean height ranges are similar to those for θ in (9) but for individual profiles they often differ.

3.3. *Results for Regional Surface Fluxes*

Linear regression by means of (7) and (8) of all profiles over their respective ranges, determined in section 3.2, yielded values of the surface fluxes. These fluxes, which are denoted H_p and LE_p, are compared in Figures 5 and 6 with the corresponding fluxes H_s and LE_s measured at the eddy correlation station. In Figure 5 the mean slope through the origin is $H_s/H_p = 0.97$ and the correlation coefficient is $r = 0.75$. In Figure 6 these results are $LE_s/LE_p = 0.96$ and $r = 0.66$.

The evaporation rate can also be estimated from H by means of the energy budget

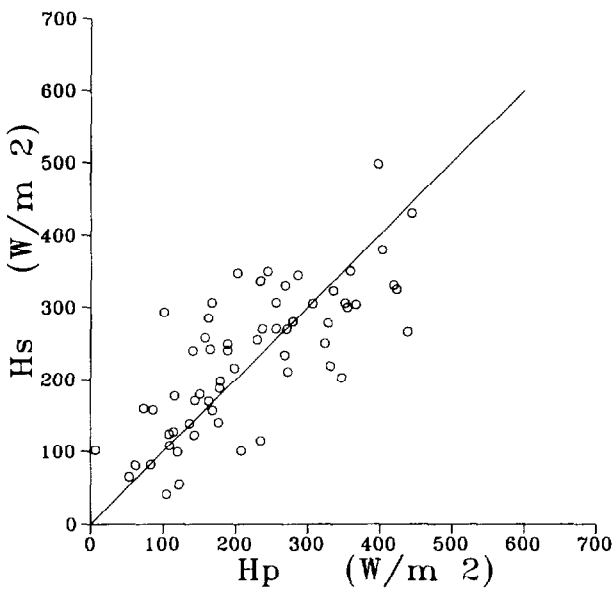

Fig. 5. Comparison between sensible heat flux values H_p derived from potential temperature profiles by means of (7) on the basis of Monin-Obukhov similarity and the values H_s measured with an eddy correlation system at 9 m above the forest canopy some 4.5 km away from the corresponding site. The mean slope through the origin is 0.97, and the correlation coefficient $r = 0.75$.

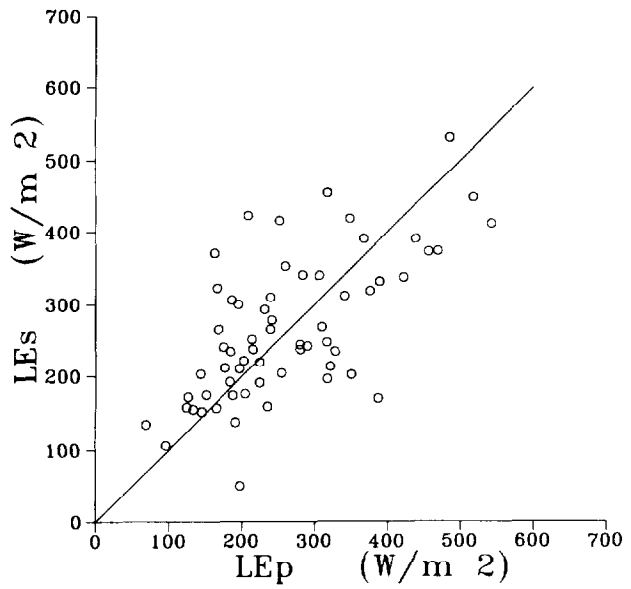

Fig. 6. Comparison between latent heat flux values LE_p derived from specific humidity profiles by means of (8) on the basis of the Monin-Obukhov similarity and the values LE_s measured with an eddy correlation system at 9 m above the treetops some 4.5 km away from the radiosounding site. The mean slope through the origin is 0.96, and $r = 0.66$.

$$LE = R_n - G - H \tag{13}$$

where R_n is the net radiation and G is the heat flux into the ground (or other substrate). Figure 7 shows a comparison between LE_s and LE obtained from (13) in which $(R_n - G)$ was taken as $(H_s + LE_s)$ (to eliminate possible error in the R_n and G estimates) and H as H_p. The mean ratio is $LE_s/LE = 0.91$ and the correlation is $r = 0.82$.

The profile-derived fluxes were also compared with the corresponding surface fluxes measured in the agricultural fields in the clearing. For H_p the correlation coefficients were $r =$ 0.49 with the fluxes from the oats and $r = 0.53$ with those from the maize. For LE_p they were lower ($r < 0.3$). Therefore these results are not presented here. They do confirm, however, the earlier finding that in the Landes Region the forested areas dominate the regional land surface–atmospheric interaction.

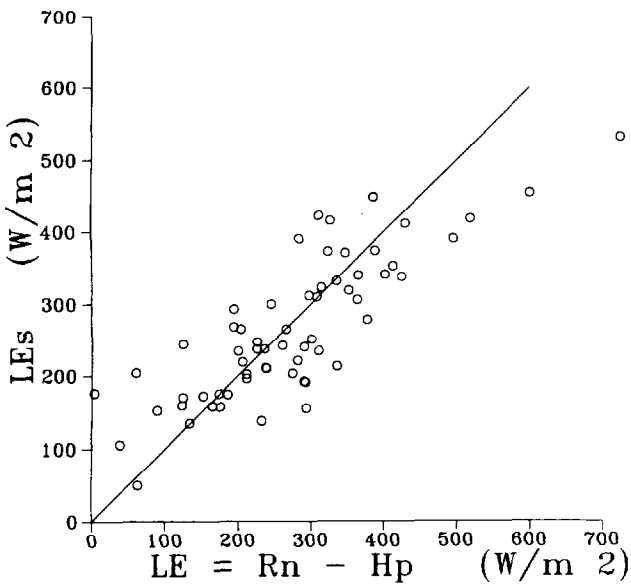

Fig. 7. Comparison between latent heat flux values obtained by means of the energy budget and LE_s measured by the eddy correlation method. The mean slope through the origin is 0.91 and $r = 0.82$.

3.4. *Discussion of Results*

The height ranges shown in (9)–(12) were obtained by inspection of each profile by applying "rules" to ensure realistic flux values. Clearly, for any given profile the points chosen this way do not necessarily represent the best section over which the Monin-Obukhov similarity with (5) is valid. In order to check this the height range for each profile was also determined by selecting that set of contiguous points for which the profile-derived flux was closest to the value measured at the eddy correlation station. For the potential temperature the result for 62 flights was

$$41(\pm 30) \leq (z - d_0)/z_0 \leq 130(\pm 49) \tag{14}$$

and for the specific humidity the result was

$$48(\pm 36) \leq (z - d_0)/z_0 \leq 153(\pm 63) \tag{15}$$

which are similar to (10)–(13). Naturally, the fluxes H_p and LE_p obtained this way are closer to H_s and LE_s, respectively, than those shown in Figures 5 and 6. For sensible heat flux the mean slope through the origin is $H_s/H_p = 1.0$ and $r = 0.86$. For evaporation the mean slope is $LE_s/LE_p = 0.98$ and $r = 0.78$.

As shown in (10) and (12) (or (14) and (15)), the mean lower limit $(z - d_0)$ obtained for the surface sublayer is of the order of 40 to 50 z_0. This is roughly the same height as that (namely, 60 z_0) obtained in the analysis of the corresponding unstable wind speed profiles by *Parlange and Brutsaert* [1992] and that (namely, 43 z_0) obtained for the neutral humidity profiles by *Brutsaert et al.* [1989]. It is also in good agreement with values obtained in experiments at nonforested sites. For neutral humidity profiles in the rugged Swiss Fore-Alps, where $z_0 = 3.8$ m and $d_0 = 46$ m, *Brutsaert and Kustas* [1985] found 50 z_0; in the Flint Hills prairie region in northeastern Kansas, where $z_0 = 1.05$ m and $d_0 = 26.9$ m, the lower limit was 52 z_0 for the neutral humidity profiles [*Brutsaert et al.*, 1991], 45 z_0 for the unstable potential temperature profiles, and 42 z_0 for the unstable humidity profiles [*Brutsaert and Sugita*, 1990; *Sugita and Brutsaert*, 1992]. Although one might have some reservations about these results, because the measurements were all made with radiosondes, they are consistent with earlier observations of the logarithmic velocity profile in wind tunnels [e.g., *Townsend*, 1976, pp. 139–143; *Raupach et al.*, 1980].

Similarly, in the light of the potential sampling problem associated with the rapid (approximately 1 min) rise of radiosondes through the lower ABL, it would seem almost fortuitous that the fluxes could be estimated as well as illustrated in Figures 5, 6, and 7. Indeed, each measured profile is but one realization of an irregular stochastic process of turbulent flow; this is probably the main reason why the height ranges vary so much from one profile to the next. Small-scale turbulence certainly seems to be one of the causes for the erratic appearance of the profiles. On the other hand, however, there must be considerable smoothing of the observed profiles in the process of the least squares regression fit with the Monin-Obukhov, equations (7) and (8), through the data. This undoubtedly compensates for local deviations and short-time turbulent

fluctuations. Thus the large-scale mixing of the fluxes from the land surface is still reflected in the mean slopes of the regression. Moreover, the means of the ranges, as presented in (9)–(12), probably are quite close to the ensemble averages for these individual realizations. A final point in support of the present findings with radiosondes is our earlier study [*Parlange and Brutsaert*, 1990]; this showed that wind profiles measured by radiosondes are at least as reliable, to determine z_0 and the surface momentum flux u_*, as those measured by a sodar system with turbulence averaging times of 15 min.

4. Conclusions

Regression analysis of temperature and humidity profiles measured by radiosondes by means of Monin-Obukhov similarity can be used to estimate regional surface fluxes of sensible and latent heat from forest. For evaporation, better results were obtained with temperature profiles and the energy budget than with the corresponding humidity profiles (Figures 6 and 7). The forest was quite nonuniform, and 35% of the general area consisted of clearings. Evidently, because the horizontal scales of the heterogeneities did not exceed approximately 10^3 m, the surface could be considered quasi-uniform from the regional point of view. The Businger-Dyer formulation for the scalar profiles was found to give a good representation of the similarity functions.

It was possible to establish a procedure to determine for most of the profiles the height range of the inner region over which surface layer similarity can be applied. Potential temperature is a better tracer in this regard than specific humidity, as the outer region is more strongly manifested by the change in slope of the θ profile. The present findings regarding the lower height limit of the surface sublayer above the Landes Forest are consistent with previous findings, when scaled as $(z - d_0)/z_0$. Thus these results do not support the notion that the turbulent transport characteristics of tall trees and forest are anomalous compared to those of surfaces with small values of z_0, even in wind tunnels.

Acknowledgments. The authors are grateful to J. C. André and J. P. Goutorbe, of the CNRM in Toulouse, and to A. Perrier, of the INRA in Grignon, France, without whose inspiration and leadership the experiment for this study would not have been possible. They would also like to express their thanks to the members of the 4-M team of CNRM and others who were their helpful companions on the field crew. In addition, they would like to thank J. H. C. Gash, C. R. Lloyd, and W. J. Shuttleworth of the Institute of Hydrology, Wallingford, England, who provided the eddy correlation flux data, allowing the comparisons in Figures 5, 6, and 7. This research has been supported and financed, in part, by the Division of Atmospheric Sciences of the National Science Foundation through grant ATM-8601115, by the National Aeronautics and Space Administration (NAG5-1378 and NAS5-31723), and by the University of California Water Resources Center.

References

André, J.-C., J.-P. Goutorbe, and A. Perrier, HAPEX-MOBILHY: A hydrologic atmospheric experiment for the study of water budget and evaporation flux at the climatic scale, *Bull. Am. Meteorol. Soc.*, *67*, 138–144, 1986.

André, J.-C., et al., Evaporation over land-surfaces: First results from HAPEX-MOBILHY special observing period, *Ann. Geophys.*, *6*, 477–492, 1988.

Brutsaert, W., Stability correction functions for the mean wind speed and temperature in the unstable surface layer, *Geophys. Res. Lett.*, *19*, 469–472, 1992.

Brutsaert, W., and W. P. Kustas, Evaporation and humidity profiles for neutral conditions over rugged hilly terrain, *J. Appl. Meteorol.*, *24*, 915–923, 1985.

Brutsaert, W., and M. Sugita, The extent of the unstable Monin-Obukhov layer for temperature and humidity above complex hilly grassland, *Boundary Layer Meteorol.*, *51*, 383–400, 1990.

Brutsaert, W., M. B. Parlange, and J. H. C. Gash, Neutral humidity profiles in the boundary layer and regional evaporation from sparse pine forest, *Ann. Geophys.*, *7*, 623–630, 1989.

Businger, J., A note on the Businger-Dyer profiles, *Boundary Layer Meteorol.*, *42*, 145–151, 1988.

Dyer, A. J., A review of flux-profile relationships, *Boundary Layer Meteorol.*, *7*, 363–372, 1974.

Garratt, J. R., Flux profile relations above tall vegetation, *Q. J. R. Meteorol. Soc.*, *104*, 199–211, 1978.

Garratt, J. R., Comments on "Analysis of the flux-profile relationships above tall vegetation—An alternative view," *Q. J. R. Meteorol. Soc.*, *105*, 1079–1082, 1979.

Garratt, J. R., Surface influence upon vertical profiles in the atmospheric near-surface layer, *Q. J. R. Meteorol. Soc.*, *106*, 803–819, 1980.

Gash, J. H. C., W. J. Shuttleworth, C. R. Lloyd, J. C. André, J. P. Goutorbe, and J. Gelpe, Micrometeorological measurements in Les Landes Forest during HAPEX-MOBILHY, *Agric. For. Meteorol.*, *46*, 131–147, 1989.

Hicks, B. B., G. D. Hess, and M. L. Wesely, Analysis of flux-profile relationships above tall vegetation—An alternative view, *Q. J. R. Meteorol. Soc.*, *105*, 1074–1077, 1979.

Högström, U., Non-dimensional wind and temperature profiles in the atmospheric surface layer: A re-evaluation, *Boundary Layer Meteorol.*, *42*, 55–78, 1988.

Kader, B. A., and A. M. Yaglom, Mean fields and fluctuation moments in unstably stratified turbulent boundary layers, *J. Fluid Mech.*, *212*, 637–662, 1990.

Monin, A. S., and A. M. Obukhov, Basic laws of turbulent mixing in the ground layer of the atmosphere (in Russian), *Trudy Geofiz. Inst. Akad. Nauk SSSR*, *24*(151), 163–187, 1954. (German translation, Sammelband zur Statistischen Theorie der Turbulenz, edited by H. Goering, 228 pp., Akademie Verlag, Berlin, 1958.)

Parlange, M. B., and W. Brutsaert, Regional roughness of the Landes Forest and surface shear stress under neutral conditions, *Boundary Layer Meteorol.*, *48*, 69–81, 1989.

Parlange, M. B., and W. Brutsaert, Are radiosonde time scales appropriate to characterize boundary layer wind profiles?, *J. Appl. Meteorol.*, *29*, 249–255, 1990.

Parlange, M. B., and W. Brutsaert, Regional shear stress of broken forest from radiosonde wind profiles in the unstable surface layer, *Boundary Layer Meteorol.*, in press, 1992.

Raupach, M. R., Anomalies in flux-gradient relationships over forest, *Boundary Layer Meteorol.*, *16*, 467–486, 1979.

Raupach, M. R., J. B. Stewart, and A. S. Thom, Comments on "Analysis of flux-profile relationships above tall vegetation—An alternative view," *Q. J. R. Meteorol. Soc.*, *105*, 1077–1078, 1979.

Raupach, M. R., A. S. Thom, and I. Edwards, A wind-tunnel study of turbulent flow close to regularly arrayed rough surfaces, *Boundary Layer Meteorol.*, *18*, 373–397, 1980.

Shuttleworth, W. J., Micrometeorology of temperate and tropical forest, *Philos. Trans. R. Soc. London, Ser. B*, *324*, 299–334, 1989.

Sugita, M., and W. Brutsaert, The stability functions in the bulk similarity formulation for the unstable boundary layer, *Boundary Layer Meteorol.*, in press, 1992.

Thom, A. S., J. B. Stewart, H. R. Oliver, and J. H. C. Gash, Comparison of aerodynamic and energy budget estimates of fluxes over a pine forest, *Q. J. R. Meteorol. Soc.*, *101*, 93–105, 1975.

Townsend, A. A., *The Structure of Turbulent Shear Flow*, 2nd ed., 429 pp., Cambridge University Press, New York, 1976.

W. Brutsaert, School of Civil and Environmental Engineering, Hollister Hall, Cornell University, Ithaca, NY 14853.

M. B. Parlange, Department of Land, Air, and Water Resources, Veihmeyer Hall, University of California, Davis, CA 95616.

(Received May 10, 1991;
revised July 30, 1992;
accepted August 5, 1992.)